

enough to compensate for the longer Ge-CH<sub>3</sub> distance as found in the crystal.

**Acknowledgment.** The authors gratefully acknowledge the financial support given this work by the National Foundation through Grants GP-20723 and GY-9498.

**Registry No.** Me<sub>3</sub><sup>76</sup>Ge<sup>12</sup>C<sup>14</sup>N, 51015-78-2; Me<sub>3</sub><sup>74</sup>Ge<sup>12</sup>C<sup>14</sup>N, 51015-79-3; Me<sub>3</sub><sup>72</sup>Ge<sup>12</sup>C<sup>14</sup>N, 51015-80-6; Me<sub>3</sub><sup>70</sup>Ge<sup>12</sup>C<sup>14</sup>N, 51065-33-9; Me<sub>3</sub><sup>76</sup>Ge<sup>13</sup>C<sup>14</sup>N, 51015-81-7; Me<sub>3</sub><sup>74</sup>Ge<sup>13</sup>C<sup>14</sup>N, 51015-82-8; Me<sub>3</sub><sup>72</sup>Ge<sup>13</sup>C<sup>14</sup>N, 51015-83-9; Me<sub>3</sub><sup>70</sup>Ge<sup>13</sup>C<sup>14</sup>N, 51015-84-0; Me<sub>3</sub><sup>76</sup>Ge<sup>12</sup>C<sup>15</sup>N, 51015-85-1; Me<sub>3</sub><sup>74</sup>Ge<sup>12</sup>C<sup>15</sup>N, 51015-86-2; Me<sub>3</sub><sup>72</sup>Ge<sup>12</sup>C<sup>15</sup>N, 51015-87-3; Me<sub>3</sub><sup>70</sup>Ge<sup>12</sup>C<sup>15</sup>N, 51015-88-4; trimethylcyano-germane, 7293-42-7.

Contribution from the Department of Chemistry and Division of Engineering, Brown University, Providence, Rhode Island 02912

## Preparation and Characterization of Some CoXY Compounds Where X = P, As, Sb and Y = S, Se<sup>1</sup>

H. NAHIGIAN, J. STEGER, H. L. MCKINZIE, R. J. ARNOTT, and A. WOLD\*

Received October 29, 1973

AIC30796\*

The lattice parameters for the CoXY series of compounds where X = P, As, Sb and Y = S, Se were determined. CoPS is tetragonal, CoAsS is cubic, CoSbS and CoPSe are orthorhombic, and CoAsSe and CoSbSe are "anomalous" marcasites. Partial ordering of As-S pairs was found for ground single crystals of CoAsS. Magnetic measurements made on the CoXY type compounds showed weak, temperature-independent paramagnetism except for CoSbS, which was diamagnetic. Electrical data indicate that the specific anion appears to affect the nature of the electrical properties.

### Introduction

A number of recent studies have described the preparation and properties of anion-substituted cobalt chalcogenides.<sup>2-5</sup> Some of these studies have been concerned with the electrical, magnetic, and crystallographic characterization of the CoXY materials (Table I), where X is a pnictide and Y is the chalcogenide.<sup>6-11</sup> However, the more general problem of the properties of these materials as a class has not been considered.

CoPS was first reported by Hulliger<sup>6</sup> to be cubic with a cell edge  $a = 5.422$  Å. However, close examination of CoPS diffractometer patterns<sup>5</sup> revealed a splitting of all peaks requiring an indexing on the basis of a tetragonal unit cell.

CoAsS has been observed to crystallize in both a high- and low-temperature form.<sup>7</sup> The high-temperature pyrite phase is indicative of a random distribution of the anions throughout the structure. The low-temperature form shows additional reflections not allowed in the pyrite space group  $Pa\bar{3}$ . The additional reflections are believed to be due to anion ordering. Two models have been proposed for this low-temperature form. Onerato<sup>8</sup> has suggested a monoclinic crystal structure (space group  $P2_1/b$ ) characterized by an ordered anion substitution of alternating As-As, S-S pairs in a series of lattice planes perpendicular to the  $a$  crystallographic axis (Figure 1). Giese and Kerr<sup>7</sup> have studied mineral samples of CoAsS (cobaltite) and reported a high-temperature

pyrite form in the 800-850° range. They also reported that some CoAsS samples showed anion ordering consistent with the orthorhombic  $Pca2_1$  space group. Such an ordered structure would have a spatial arrangement containing As-S pairs in a series of lattice planes as shown in Figure 2.

Both synthetic and naturally occurring CoSbS (paracostibite) are orthorhombic and give a set of reflections similar to those of  $\alpha$ -NiAs<sub>2</sub> (pararammelsbergite). Hence, CoSbS may have a structure similar to that of  $\alpha$ -NiAs<sub>2</sub><sup>12,13</sup> which is intermediate between that of pyrite and marcasite. In the pyrite structure all the corners of each cation octahedron share corners with two neighboring octahedra. This results in a total sharing of each octahedron with 12 neighboring octahedra (Figure 3). In the marcasite structure each octahedron shares two parallel and opposite edges with two neighboring octahedra and corners with an additional eight neighboring octahedra (Figure 4). The combination of both the pyrite and marcasite stacking sequence of the octahedra results in the  $\alpha$ -NiAs<sub>2</sub> structure. In this structure each octahedron shares an edge with one neighboring octahedron and corners with ten additional neighboring octahedra.

CoAsSe has been reported by Hulliger<sup>6</sup> to crystallize as a cubic pyrite (space group  $Pa\bar{3}$ ) with a cell edge of  $a = 5.76$  Å. There have been no previous X-ray studies reported for either CoPSe or CoSbSe.

In order to correlate the effects of anion substitution on the transport and magnetic properties of CoS<sub>2</sub> and CoSe<sub>2</sub>, a systematic study of CoXY type compounds (X = P, As, Sb and Y = S, Se) was initiated.

### Experimental Section

Polycrystalline samples of all compositions were prepared directly from the elements in evacuated silica tubes. (Spectroscopic grade Co, P, As, Se, and S were obtained from Atomergic Chemical Co., Division of Gallard-Schlesinger Chemical Corp., New York, N. Y.) Samples were given three heat treatments (800-850°) and two intermediate grindings under a dry nitrogen atmosphere. The

(1) This work was supported by the U. S. Army Research Office, Durham, N. C.

(2) V. Johnson and A. Wold, *J. Solid State Chem.*, **2**, 209 (1970).

(3) (a) K. Adachi, K. Sato, and M. Takeda, *J. Phys. Soc. Jap.*, **26**, 631 (1969); (b) K. Adachi, K. Sato, and M. Matsuura, *ibid.*, **29**, 323 (1970).

(4) J. Mikkelsen and A. Wold, *J. Solid State Chem.*, **3**, 39 (1971).

(5) H. Nahigian, J. Steger, R. J. Arnett, and A. Wold, to be submitted for publication.

(6) F. Hulliger, *Nature (London)*, **198**, 382 (1963).

(7) R. F. Giese, Jr., and P. F. Kerr, *Amer. Mineral.*, **50**, 1002 (1965).

(8) E. Onerato, *Acta Crystallogr.*, **10**, 764 (1957).

(9) F. Hulliger, *Helv. Phys. Acta*, **35**, 535 (1962).

(10) L. J. Cabri, D. C. Harris, and J. M. Stewart, *Can. Mineral.*, **10**, 232 (1970).

(11) F. Hulliger and E. Mooser, *J. Phys. Chem. Solids*, **26**, 429 (1965).

(12) W. Stassen and R. D. Heyding, *Can. J. Chem.*, **46**, 2159 (1968).

(13) M. E. Fleet, *Amer. Mineral.*, **57**, 1 (1972).

Table I. Some Previous Studies of the Ternary Cobalt Pnictide Substituted Chalcogenides

Compd	Crystallography	Lattice parameters, Å	Specimen type	Electrical properties	Magnetic properties
CoPS	Cubic $Pa3^6$	$a = 5.422^6$	Synth <sup>6,11</sup>	Semiconducting <sup>6</sup>	$\mu = 0^{11}$
CoAsS	Tetragonal <sup>5</sup>	$a = 5.414, c = 5.430^5$	Synth <sup>5</sup>	Semiconducting <sup>4,6</sup>	$\mu = 0^{4,11}$
	Cubic $Pa3^{4,6,7}$	$a = 5.578^6$	Mineral <sup>7</sup>		
	Orthorhombic $Pca2_1^7$	$a = 5.577^4$	Synth <sup>6,4,11</sup>		
CoSbS	Monoclinic $P2_1/b^8$	$a = 5.768, b = 5.949,$ $c = 11.666^a$	Synth and Mineral <sup>9,10</sup>	Nonmetallic <sup>9</sup>	
	Orthorhombic $Pbca^{10}$				
CoPSe	Cubic $Pa3^6$	$a = 5.76^6$	Synth <sup>6</sup>	Semiconducting <sup>6,11</sup>	$\mu = 0^{11}$
CoAsSe					
CoSbSe					

<sup>a</sup> Hulliger in a private communication to Cabri which was subsequently published by Cabri<sup>10</sup> gave orthorhombic lattice parameters  $a = 5.840$  Å,  $b = 5.958$  Å, and  $c = 11.673$  Å.

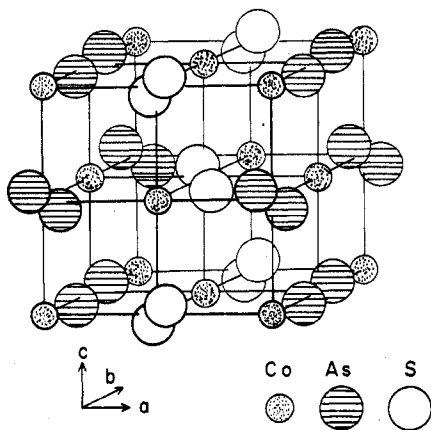
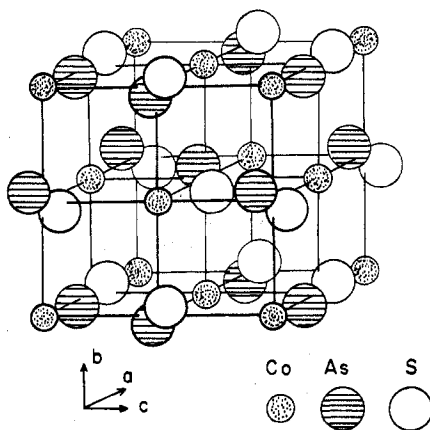
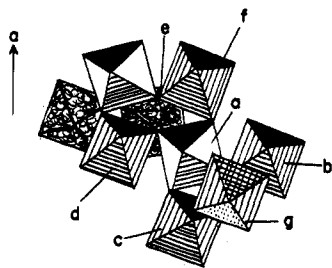
Figure 1. Monoclinic CoAsS model.<sup>7</sup>Figure 2. Orthorhombic CoAsS model.<sup>8</sup>

Figure 3. Octahedron a sharing corners with octahedra b, c, d, e, f, and g (shown) and six additional octahedra (not shown).

samples were kept at elevated temperatures for periods of 2–4 weeks. Reaction completeness was determined by both microscopic observation and X-ray analysis. Complete reaction was easier to obtain if the temperature gradient across the length of the sample tube was less than 5°.

Single crystals of all compositions, except CoPSe, were prepared by chemical vapor transport using 50–100 Torr of chlorine as a

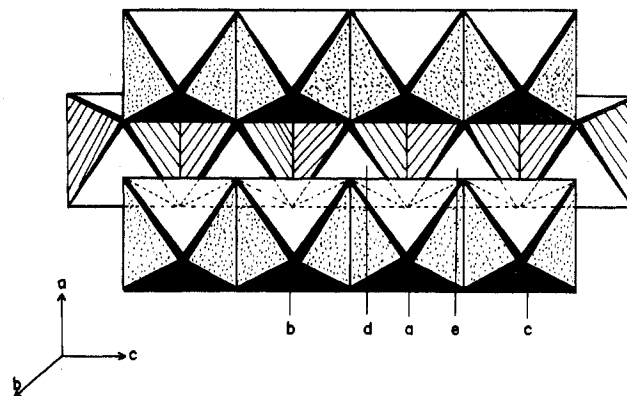


Figure 4. Octahedron a sharing edges with octahedra b and c and corners with octahedra d and e (shown) and octahedron a also sharing corners with six additional octahedra (not shown).

transporting agent. The distance between charge and growth zones was approximately 12.5 cm. Details of the actual growth temperature conditions are given in Table II. Single crystals rather than polycrystalline materials were used for magnetic and electrical measurements because of greater crystallinity and homogeneity.

**Sample Characterization. X-Ray Diffraction.** Powder diffraction patterns were obtained with a Norelco diffractometer using monochromated high-intensity  $\text{Cu K}\alpha_1$  radiation ( $\lambda 1.5405$  Å). Diffraction scans ( $0.25^\circ/\text{min}$ ) were obtained for all samples from  $12^\circ < 2\theta \leq 130^\circ$ . Lattice parameters were determined by a least-squares refinement of high-angle reflections ( $60^\circ \leq 2\theta \leq 130^\circ$ ) relative to a silicon standard. Room-temperature intensity data for ordered CoAsS samples were collected by accumulating counts while scanning ( $0.25^\circ/\text{min}$ ) over each reflection. The background intensities were obtained from a curve constructed from background readings taken in regions not having any interfering peaks. These background values were subtracted from the total intensity values for each peak. Refinement of two variable atomic position parameters, the unit cell temperature factor, and the variable occupancy factor was accomplished using a Fortran program that minimized the discrepancy factor

$$R = \frac{100 \sum |I_i^{\text{calcd}} - I_i^{\text{obsd}}|}{\sum I_i^{\text{obsd}}}$$

The atomic scattering factors used for  $\text{Co}^{3+}$ ,  $\text{As}^0$ , and  $\text{S}^0$  were those given by Cromer and Waber,<sup>14</sup> whereas the real and imaginary parts of the anomalous dispersion terms were obtained from Cromer.<sup>15</sup> The intensity data were corrected for the polarization caused by the curved graphite diffracted-beam monochromator.

**Density Determination.** The measured densities of all samples agreed with the theoretical densities and are reported in Table II. Sample densities were determined using a hydrostatic technique<sup>16</sup> employing a Mettler Model H 54 analytical balance. The density medium perfluoro(1-methyldecalin) was chosen because of its rela-

(14) D. T. Cromer and J. T. Waber, *Acta Crystallogr.*, **18**, 104 (1965).

(15) D. T. Cromer, *Acta Crystallogr.*, **18**, 17 (1965).

(16) R. Adams, Ph.D. Thesis, Brown University, 1973.

Table II. Growth Conditions, Crystallography, Lattice Parameters, and Densities

Compd	Chemical vapor transport		Direct combination temp, °C	Crystallography	Lattice parameters, Å	$\rho$ , g/cm <sup>3</sup>	
	Charge zone, °C	Growth zone, °C				Calcd	Exptl
CoPS	925	875	850	Tetragonal	$a = 5.414$ (5) $c = 5.430$ (5)	5.077	5.07 (2)
CoAsS(p)	825	775	800	Cubic pyrite	$a = 5.576$ (2)	6.356	6.36 (2)
CoAsS(o)	750	700		Orthorhombic	$a = b = c = 5.576$ (2)	6.356	6.36 (2)
CoSbS	890	790	775	Orthorhombic	$a = 5.834$ (9) $b = 5.953$ (5) $c = 11.664$ (5)	6.978	6.96 (2)
CoPSe			775	Orthorhombic	$a = 5.548$ (9) $b = 5.659$ (5) $c = 11.185$ (5)	6.331	6.31 (2)
CoAsSe	825	775	800	Orthorhombic marcasite	$a = 4.751$ (5) $b = 5.753$ (5) $c = 3.584$ (5)	7.247	7.26 (2)
CoSbSe	890	790	775	Orthorhombic marcasite	$a = 5.056$ (5) $b = 6.031$ (5) $c = 3.686$ (5)	7.676	7.67 (2)

Table III. Electrical and Magnetic Properties of Single Crystals at Room Temperature

Compd	$n$ , <sup>a</sup> carriers/ g-atom of Co	$\rho$ , $\Omega$ cm	$R_H$ , cm <sup>3</sup> /C	$\mu$ , <sup>b</sup> cm <sup>2</sup> / V sec	$E_g$ , eV	Carrier type	$10^6 \chi_M$ , <sup>d</sup> cgsu/mol
CoPS		$7.15 \times 10^{-3}$	$3.39 \times 10^{-3}$			n	+21
CoAsS		$1.49 \times 10^{-1}$	$1.17 \times 10^{-2}$		$\approx 0.05$	n	+11
CoSbS		1.12	3.65		0.11	n	-2
CoPSe <sup>c</sup>							+15
CoAsSe <sup>d</sup>	$1.23 \times 10^{23}$	$4.57 \times 10^{-4}$	$1.64 \times 10^{-3}$	3.6		n	+27
CoSbSe <sup>d</sup>	$4.03 \times 10^{23}$	$8.83 \times 10^{-4}$	$5.25 \times 10^{-4}$	0.59		n	+82

<sup>a</sup> Certain values of  $n$  and  $\mu$  were not reported because of the possible presence of both p- and n-type carriers. <sup>b</sup> The mobility was calculated using the equation  $\mu = R_H/\rho$ . <sup>c</sup> Powder sample. <sup>d</sup> Values reported are temperature independent.

tively low vapor pressure and its ability to wet the samples. A high-purity silicon crystal ( $\rho = 2.328$  g/cm<sup>3</sup>) was chosen for calibrating the density liquid. In order to obtain reproducible results, care was taken to outgas the samples thoroughly prior to density measurements.

**Electrical and Magnetic Measurements.** Electrical measurements included resistivity and Hall and Seebeck effects. Indium leads for the electrical measurements were attached to crystals by means of an ultrasonic soldering technique.<sup>17</sup> Crystals were small and irregularly shaped so that only the van der Pauw method<sup>18</sup> could be used. All electrical measurements were made according to the method described by Lee, *et al.*<sup>17</sup>

Magnetic measurements were made on single crystals using a Faraday balance as described by Morris and Wold.<sup>19</sup> The absence of a significant amount of ferromagnetic impurities was verified by the Honda-Owen method.<sup>20</sup> No corrections were made for core diamagnetism because of the large uncertainty in the magnitude of the corrections relative to the magnitude of the susceptibility values for various crystals studied. The results of both the electrical and magnetic measurements are given in Table III.

## Results and Discussion

**Crystallography.** Several different crystal structures result from the pnictide substitution of both cobalt disulfide and diselenide. The pertinent crystallographic results are given in Table II. All structures discussed exhibit the same two types of coordination; *i.e.*, cobalt is octahedrally coordinated by six anions and each anion is tetrahedrally coordinated by three cations and one anion. As has been reported, two forms of CoAsS were observed. Those samples prepared in the 800–850° range gave a normal pyrite X-ray pattern. However, those samples prepared in the range 700–800° showed additional reflections forbidden by the pyrite  $Pa3$  space group. In order to distinguish between the

Onerato and Giese and Kerr models for the latter materials, powder intensity data were collected for a "low-temperature" ( $T < 800^\circ$ ) sample of CoAsS. These data were used to refine four independent parameters: two anion positions, isotropic cell temperature factor, and anion occupancy factor. Intensity calculations were performed on the basis of both the monoclinic (Onerato<sup>8</sup>) and orthorhombic (Giese and Kerr<sup>7</sup>) models. The models of Onerato and Giese and Kerr were based on the premise that anion pairs of the low-temperature form of CoAsS were completely ordered. However, in the present study, the degree of anion order was allowed to vary in order to optimize the correlation between observed and calculated data. For the orthorhombic structure the best correlation was obtained with 58% of the anions ordered (ordered X-Y pairs). The final values for the variable parameters are tabulated in Table IV. Table IV shows that the calculated intensities based on the orthorhombic structure were closer to the observed values than those calculated for the monoclinic model. The reliability factor  $R$ , which indicates the degree of correlation between the calculated and observed intensities, was 0.122 and 0.077 for the monoclinic and orthorhombic structures, respectively. From Table IV it can be seen that the 200 and 400 reflections show more substantial differences between observed and calculated intensities than other reflections of the data set. The 200 and 400 planes are parallel to the {100} cleavage, which suggests preferred orientation of these planes, even after extensive grinding. An improved  $R$  factor (0.048) resulted when the 200 and 400 reflections were eliminated from the orthorhombic data set. The anion arrangement of the ordered CoAsS structure has As-S pairs in a stacking sequence AsS/SAs/AsS/. . . when looking along the  $b$  axis (Figure 2).

CoAsSe and CoSbSe both crystallized with the marcasite structure (orthorhombic space group  $Pnn2$ ). The reliability

(17) H. N. S. Lee, H. McKinzie, D. S. Tannhauser, and A. Wold, *J. Appl. Phys.*, **42**, 602 (1969).

(18) L. J. Van der Pauw, *Philips Res. Rep.*, **13**, 1 (1958).

(19) B. Morris and A. Wold, *Rev. Sci. Instrum.*, **39**, 1937 (1968).

(20) L. F. Bates, "Modern Magnetism," Cambridge University Press, New York, N. Y., 1961.

Table IV. Observed and Calculated Intensities for CoAsS

Cubic $hkl$	$I_{\text{obsd}}$	Orthorhombic $hkl$	$I_{\text{calcd}}$	Monoclinic $hkl$	$I_{\text{calcd}}$
100	4.33	010	4.54	100	3.35
110	2.42	110	2.56	101, 011, $\bar{1}01$	4.21
111	6.17	111	9.48	111, $\bar{1}\bar{1}\bar{1}$	6.71
200	74.7	200, 002, 020	58.90	002, 020, 200	56.19
210 <sup>a</sup>	100.00	021, 210, 201, 120	103.30	120, 102, 012, 021, 201, $\bar{1}02$ , $\bar{2}01$	116.93
211 <sup>a</sup>	85.40	112, 121, 211	88.17	211, 121, 112, $\bar{2}\bar{1}\bar{1}$ , $\bar{1}\bar{2}\bar{1}$ , $\bar{1}\bar{1}\bar{2}$	90.85
220	28.00	220, 202, 022	30.32	022, 202, 220, $\bar{2}02$	26.42
221	2.94	030, 221, 212, 122	2.79	300, 122, 212, 221, $\bar{1}\bar{2}\bar{2}$ , $\bar{2}\bar{1}\bar{2}$ , $\bar{2}\bar{2}\bar{1}$	1.86
310	0.96	310, 130	0.74	013, 031, 103, 301, $\bar{3}01$ , $\bar{1}03$	1.15
311 <sup>a</sup>	90.30	311, 113, 131	92.71	113, 131, 311, $\bar{1}\bar{1}\bar{3}$ , $\bar{1}\bar{3}\bar{1}$ , $\bar{3}\bar{1}\bar{1}$	94.49
222	8.98	222	9.95	222, $\bar{2}\bar{2}\bar{2}$	10.25
230	30.70	203, 320, 230, 032	33.38	023, 032, 203, 302, 320, $\bar{2}03$ , $\bar{3}02$	29.03
231	47.3	312, 213, 123, 321, 231, 132	47.49	123, 132, 231, 213, 312, 321, 123, $\bar{1}\bar{3}\bar{2}$ , $\bar{2}\bar{3}\bar{1}$ , $\bar{2}\bar{1}\bar{3}$ , $\bar{3}\bar{1}\bar{2}$ , $\bar{3}\bar{2}\bar{1}$	44.72
400	7.05	400, 004, 040	4.51	004, 040, 400	4.30
410	2.35	401, 410, 140, 014, 322, 223, 232	2.45	014, 041, 104, 401, 140, 223, 232, 322, $\bar{1}04$ , $\bar{4}01$ , $\bar{2}\bar{2}\bar{3}$ , $\bar{2}\bar{3}\bar{2}$ , $\bar{3}\bar{2}\bar{2}$	0.89
411	1.46	411, 114, 141, 330	1.06	114, 141, 411, 033, 303, $\bar{1}\bar{1}\bar{4}$ , $\bar{1}\bar{4}\bar{1}$ , $\bar{4}\bar{1}\bar{1}$ , $\bar{3}03$ , 133, $\bar{3}\bar{1}\bar{3}$ , 331, $\bar{3}\bar{3}\bar{1}$ , 313, $\bar{1}\bar{3}\bar{3}$	2.68

Arsenic position<sup>a</sup> = 0.379 (5); sulfur position<sup>b</sup> = 0.385 (5); occupancy factor<sup>c</sup> = 0.787 (5)

<sup>a</sup> These reflections were not used in the refinement program. <sup>b</sup> Due to the limited intensity data available, cubic  $x, x, x$  parameters were used rather than the more proper orthorhombic  $x, y, z$  parameters. <sup>c</sup> To calculate the degree of anion ordering: [(occupancy factor) - (occupancy factor for complete anion disorder (0.5))] / 0.5.

indices for the lattice parameter determinations were  $<0.05$  for both the polycrystalline and single-crystal samples. The structure appears to be that of the "anomalous" marcasite form<sup>11,21,22</sup> since the  $c/a$  and  $c/b$  axial ratios are 0.75 and 0.62 for CoAsSe and 0.73 and 0.61 for CoSbSe. In this study only the anomalous marcasite structure was formed from both direct combination and chemical vapor transport. Hulliger<sup>6</sup> reported the existence of a cubic pyrite phase for CoAsSe, but the details of his synthesis were not discussed.

CoSbS and CoPSe were both indexed on orthorhombic unit cells. The reliability factors for the lattice parameter determination were  $<0.05$ . The X-ray diffraction patterns of these compounds are similar to those of the mineral parammelsbergite, which is intermediate between the anomalous marcasites (CoAsSe and CoSbSe) and the pyrite form of CoAsS.

**Electrical and Magnetic Data.** Resistivity, Hall, and magnetic susceptibility measurements were taken over the temperature range 77–400°K (Table III). Higher temperature measurements were not made because of possible decomposition of the samples. The one-electron band model proposed by Goodenough<sup>23,24</sup> for pyrite (Figure 5) and anomalous marcasites (Figure 6) can be used as a basis for understanding the results obtained. For both the pyrite and anomalous-marcasite compounds, Goodenough has shown that for  $d \geq 6$  the bands formed from the cation  $t_{2g}$  orbitals are completely filled. With six outer d electrons, as occurs for formal valence  $\text{Co}^{3+}$ , the  $\sigma^*$ -antibonding band is empty. However, the nature of the bands for specific compounds can be altered by the character of the anions.

Resistivity measurements of CoPS over the temperature range 77–325°K indicated a slight decrease of resistivity from  $1.34 \times 10^{-2}$  to  $7.03 \times 10^{-3} \Omega \text{ cm}$ . This change in the resistivity data may reflect the extrinsic nature of the material. Pure CoPS would be expected to show semiconducting

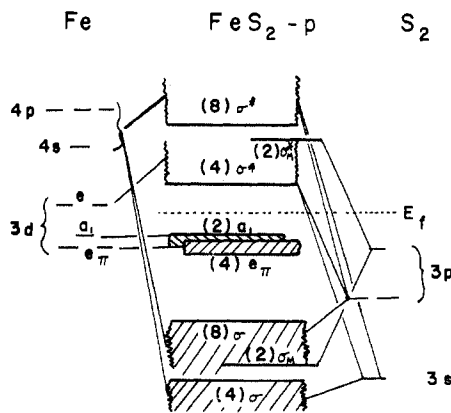


Figure 5. Energy bands for the pyrite type structure.

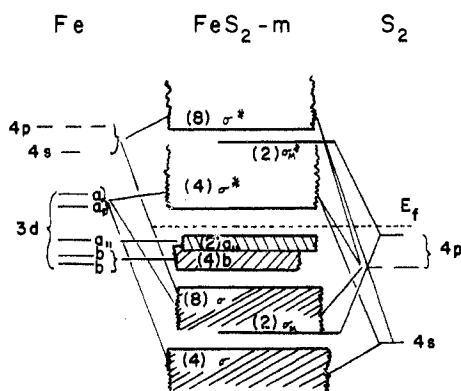


Figure 6. Energy bands for the "anomalous" marcasite structure.

behavior. A resistivity vs.  $10^3/T$  plot of the pyrite form of CoAsS indicated semiconducting behavior (Figure 7). However, only a small energy gap ( $E_g \approx 0.05 \text{ eV}$ ) was observed which may also be indicative of extrinsic behavior. [The band gap was determined from the linear portion of the  $\rho$  vs.  $10^3/T$  plot indicated in Figure 7 using the standard relation  $\rho_0/\rho = \exp(-E_g/2kT)$ .] Unfortunately, it was not possible to carry out resistivity measurements at higher temperatures because of thermal decomposition of the products. For both CoPS and CoAsS this electrical behavior and

(21) G. Bronstigen and A. Kjekshus, *Acta Chem. Scand.*, **24**, 2993 (1970).

(22) H. Holseth and A. Kjekshus, *Acta Chem. Scand.*, **22**, 3284 (1968).

(23) J. B. Goodenough, *J. Solid State Chem.*, **3**, 26 (1971).

(24) J. B. Goodenough, *J. Solid State Chem.*, **5**, 144 (1972).

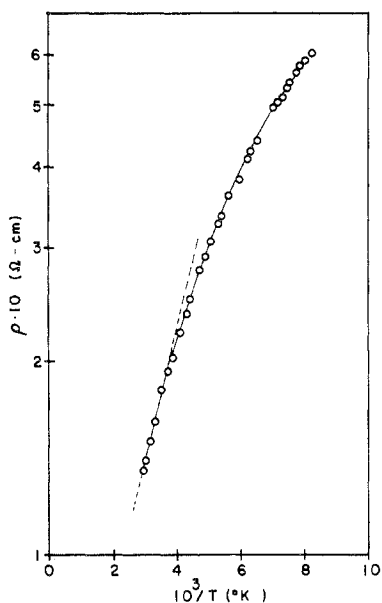


Figure 7.  $\rho$  ( $\Omega$  cm) vs.  $10^3/T$  ( $^{\circ}$ K) for CoAsS (pyrite).

associated weak temperature-independent paramagnetism [ $\chi_M \approx 10 \times 10^{-6}$  cgsu/mol for CoAsS (pyrite) and  $\chi_M \approx 21 \times 10^{-6}$  cgsu/mol for CoPS] is consistent with low-spin  $\text{Co}^{3+}$  ( $d^6$ ) in an octahedral site.

CoSbS single crystals exhibit semiconducting behavior with an energy gap of 0.11 eV (Figure 8). Susceptibility measurements from 77 to 400 $^{\circ}$ K indicate that CoSbS is diamagnetic (Figure 9). The Hall coefficient  $R_H$  vs.  $10^3/T$  is given in Figure 10 and is consistent with semiconducting behavior.

The crystal structure of CoSbS and CoPSe is not known in detail but appears similar to that of  $\alpha$ -NiAs $_2$ . In this structure the cation and anion coordination are the same as that in pyrite and the anomalous marcasite. The data show that Co is essentially low-spin  $d^6$  in both CoSbS and CoPSe.

CoAsSe and CoSbSe crystallize as anomalous marcasites, and both appear to exhibit Pauli paramagnetic behavior. In addition, they exhibit relatively higher carrier concentration and low resistivities ( $<10^{-3}$   $\Omega$  cm), as shown in Table III. It should be noted that electrical properties are extremely sensitive to the presence of impurities and the behavior observed may be extrinsic. Goodenough<sup>24</sup> proposed a band model (Figure 6) for the anomalous marcasites. He indicated the significance of the  $d_{xy}$  orbitals directed along the  $c$  axis, labeled as  $a_{||}$  in Figure 6. In the regular marcasite the  $a_{||}$  band formed from the  $a_{||}$  orbitals is empty. Covalent mixing destabilizes the  $a_{||}$  orbitals relative to the nonbonding  $d$  orbitals. In the anomalous marcasites, the  $a_{||}$  orbitals are filled and no stabilization can be achieved by covalent mixing. This suggests a probable overlap of the filled  $a_{||}$  and  $b$  bands. It has been shown<sup>25</sup> that  $\text{FeS}_2$ - $m$  (low-spin  $d^6$ ) exhibits semiconducting behavior. Since both CoAsSe and CoSbSe (low-spin  $d^6$ ) have low resistivity values and exhibit Pauli paramagnetic behavior, it is possible that the large, polarizable As, Sb, and Se anions contribute to a substantial broadening of the  $\sigma^*$  band, resulting in some overlap with the  $a_{||}$  and  $b$  bands.

### Summary

The CoXY compounds were found to exist with three closely related crystallographic structures: pyrite, para-

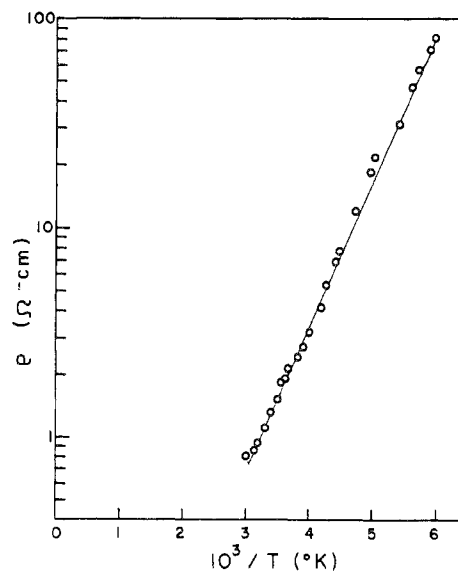


Figure 8.  $\rho$  ( $\Omega$  cm) vs.  $10^3/T$  ( $^{\circ}$ K) for CoSbS.

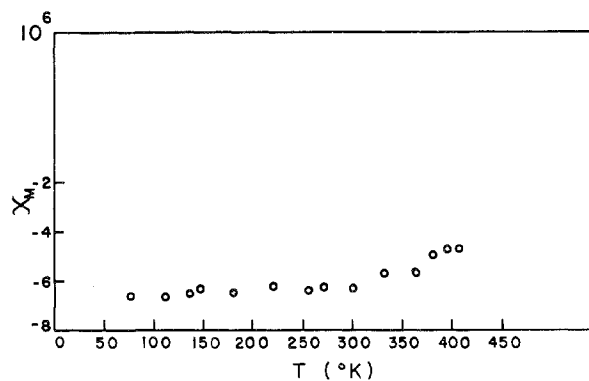


Figure 9. Susceptibility  $\chi_M$  vs. temperature ( $^{\circ}$ K) for CoSbS.

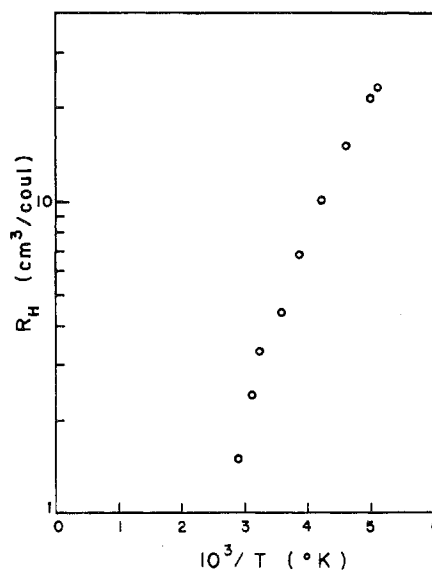


Figure 10.  $R_H$  vs.  $10^3/T$  ( $^{\circ}$ K) for CoSbS.

costibite, and anomalous marcasite. The cations are octahedrally coordinated with six anions, and the anions are tetrahedrally coordinated with three cations and one anion for all six compounds. The sharing of the edges and corners of neighboring octahedra are also related among all six compounds. CoPS is apparently a slightly distorted pyrite that could be indexed on a tetragonal unit cell. CoAsS was shown

(25) T. Bither, R. Bouchard, W. Cloud, P. Donohue, and W. Siemons, *Inorg. Chem.*, 7, 2208 (1968).

to exist as a cubic pyrite structure when prepared and quenched from 800 to 850° and as a partially ordered (orthorhombic  $Pca2_1$  space group) structure when synthesized between 700 and 800°; this partially ordered structure contained ordered As-S pairs. The compounds CoSbS and CoPSe crystallize with an orthorhombic structure, apparently similar to that of  $\alpha$ -NiAs<sub>2</sub> (pararammelsbergite). CoAsSe and CoSbSe are orthorhombic with the  $c/a$  and  $c/b$  axial ratios of the anomalous marcasite.

The temperature-independent magnetic data found for all CoXY materials studied is indicative of low-spin Co<sup>3+</sup> (d<sup>6</sup>).

The electrical data for these materials may reflect the specific effect of anions and crystallography on both the broadness and degree of separation of the valence and conduction bands.

**Acknowledgment.** The authors wish to thank Dr. J. B. Goodenough at Massachusetts Institute of Technology, Lincoln Laboratories, for helpful discussions.

**Registry No.** CoPS, 51021-56-8; CoAsS, 12254-82-9; CoSbS, 51021-58-0; CoPSe, 51021-57-9; CoAsSe, 51021-48-8; CoSbSe, 51021-59-1.

Contribution from the Department of Chemistry,  
University of British Columbia, Vancouver, Canada, V6T 1W5

## Additive Model for the Electric Field Gradient at Antimony in Some Pentacoordinate Organoantimony(V) Derivatives

JOHN N. R. RUDDICK, JOHN R. SAMS,\* and JAMES C. SCOTT

Received November 12, 1973

AIC30828T

<sup>121</sup>Sb Mossbauer data are reported for several compounds of the types Ph<sub>4</sub>SbX and Ph<sub>3</sub>SbX<sub>2</sub> (Ph = C<sub>6</sub>H<sub>5</sub>; X = various electronegative groups) and are consistent with trigonal-bipyramidal structures in which the X groups occupy one or both axial positions, respectively. The first explicit application of an additive model for the electric field gradient at Sb in organoantimony(V) compounds has been made to these and other derivatives of like stoichiometries. Calculated and observed quadrupole coupling constants ( $e^2qQ$ ) are in good agreement, indicating the adequacy of such a model for these systems. For compounds of the type Ph<sub>3</sub>SbX<sub>2</sub> there is an approximately linear relation between isomer shift ( $\delta$ ) and  $e^2qQ$ , the slope of which is consistent with  $\sigma$ -bonding effects being the dominant factor in determining the Mossbauer parameters. In derivatives containing Sb-O bonds the  $\delta$  values are more positive than would be expected on the basis of electronegativity arguments alone.

### Introduction

Additive models for the electric field gradient (efg) have been extensively employed to interpret Mossbauer quadrupole splitting data on organometallic Sn(IV) derivatives (and to a lesser extent, spin-paired Fe(II) and Fe(-II) complexes).<sup>1</sup> Such models have had considerable success in predicting both signs and magnitudes of quadrupole splittings in compounds with fairly regular geometry, although the converse application of predicting molecular geometry from measured efg parameters has met with more limited success. This is due in part to the fact that similar efg parameters may arise from two or more possible structures, so that an unequivocal choice is not always possible. Moreover, no really satisfactory method has yet been devised to account for distortions from regular geometry.

In view of the usefulness of the additive approximation for <sup>119</sup>Sn quadrupole splittings in organotin(IV) compounds it is obviously of interest to extend the treatment to <sup>121</sup>Sb quadrupole splittings in organoantimony(V) complexes, since the model should be equally applicable here.<sup>1a</sup> Although <sup>121</sup>Sb Mossbauer results for only a few organoantimony(V) derivatives have appeared in the literature, the data of Long, *et al.*,<sup>2</sup> at 4.2°K for compounds of the type R<sub>5-n</sub>SbX<sub>n</sub> (R = C<sub>6</sub>H<sub>5</sub>, CH<sub>3</sub>; X = F, Cl, Br, I; n = 0-2, but not all combinations) constitute a suitable starting point for such a treatment. In

the present paper we report <sup>121</sup>Sb Mossbauer data for several other Ph<sub>5-n</sub>SbX<sub>n</sub> (Ph = C<sub>6</sub>H<sub>5</sub>) complexes which together with the results of Long, *et al.*,<sup>2</sup> allow us to make a limited test of the additive model for <sup>121</sup>Sb quadrupole splittings.

X-Ray crystallographic studies of compounds such as Ph<sub>3</sub>SbCl<sub>2</sub>,<sup>3</sup> Me<sub>3</sub>SbCl<sub>2</sub>,<sup>4</sup> (Me = CH<sub>3</sub>), Ph<sub>4</sub>SbOMe,<sup>5</sup> Ph<sub>3</sub>Sb(OMe)<sub>2</sub>,<sup>5</sup> and Ph<sub>4</sub>SbOH<sup>6</sup> have shown that they adopt trigonal-bipyramidal structures with the electronegative groups in the axial positions. Infrared and Raman data are also consistent with this type of structure for compounds of the types R<sub>3</sub>SbX<sub>2</sub> and R<sub>4</sub>SbX.<sup>7-9</sup> There are a few exceptions such as Ph<sub>4</sub>SbClO<sub>4</sub> which is apparently ionic, but both ir<sup>8</sup> and Mossbauer<sup>2</sup> studies show when such exceptions occur. The absence of quadrupole splitting in the Mossbauer spectra (as expected for a tetrahedral Ph<sub>4</sub>Sb<sup>+</sup> cation) and the high-resonance fractions support ionic structures for both Ph<sub>4</sub>SbClO<sub>4</sub><sup>2</sup> and Ph<sub>4</sub>SbBF<sub>4</sub>.<sup>10</sup>

The structural parameters of Ph<sub>4</sub>SbOMe and Ph<sub>3</sub>Sb(OMe)<sub>2</sub>

(3) T. N. Polynova and M. A. Porai-Koshits, *J. Struct. Chem. (USSR)*, **7**, 742 (1966).

(4) A. F. Wells, *Z. Kristallogr., Kristallgeometrie, Kristallphys., Kristallchem.*, **99**, 367 (1938).

(5) K. Shen, W. E. McEwan, S. J. La Placa, W. C. Hamilton, and A. P. Wolf, *J. Amer. Chem. Soc.*, **90**, 1718 (1968).

(6) A. L. Beauchamp, M. J. Bennett, and F. A. Cotton, *J. Amer. Chem. Soc.*, **91**, 297 (1969).

(7) R. G. Goel, E. Masowsky, and C. V. Senoff, *Inorg. Chem.*, **10**, 2572 (1971).

(8) J. B. Orenberg, M. D. Morris, and T. V. Long, *Inorg. Chem.*, **10**, 933 (1971).

(9) G. G. Long, G. O. Doak, and L. D. Freedman, *J. Amer. Chem. Soc.*, **86**, 209 (1964).

(10) S. E. Gukasyan and V. S. Shpinel, *Phys. Status Solidi*, **29**, 49 (1968).

(1) See for example the recent reviews by (a) G. M. Bancroft and R. H. Platt, *Advan. Inorg. Chem. Radiochem.*, **15**, 59 (1972); (b) J. R. Sams, *MTP (Med. Tech. Publ. Co.) Int. Rev. Sci.: Phys. Chem., Ser. One*, **4**, 85 (1972).

(2) G. G. Long, J. G. Stevens, R. J. Tullbane, and L. H. Bowen, *J. Amer. Chem. Soc.*, **92**, 4230 (1970).